Journal of Materials Chemistry C

Accepted Manuscript

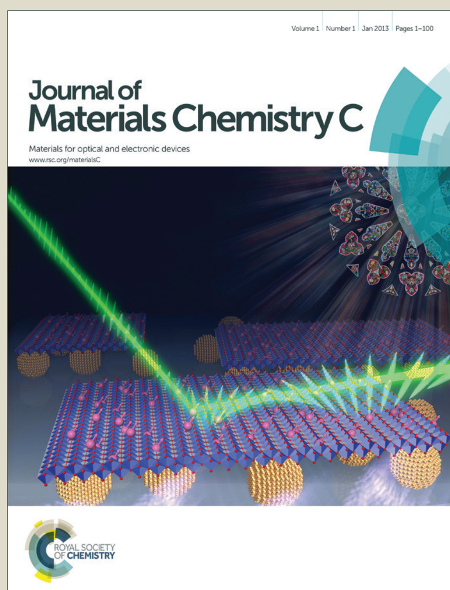

This is an *Accepted Manuscript*, which has been through the Royal Society of Chemistry peer review process and has been accepted for publication.

Accepted Manuscripts are published online shortly after acceptance, before technical editing, formatting and proof reading. Using this free service, authors can make their results available to the community, in citable form, before we publish the edited article. We will replace this *Accepted Manuscript* with the edited and formatted *Advance Article* as soon as it is available.

You can find more information about *Accepted Manuscripts* in the Information for Authors.

Please note that technical editing may introduce minor changes to the text and/or graphics, which may alter content. The journal's standard Terms & Conditions and the Ethical guidelines still apply. In no event shall the Royal Society of Chemistry be held responsible for any errors or omissions in this *Accepted Manuscript* or any consequences arising from the use of any information it contains.

ROYAL SOCIETY OF CHEMISTRY

www.rsc.org/materialsC

CREATED USING THE RSC LaTeX PCCP ARTICLE TEMPLATE – SEE www.rsc.org/electronicfiles FOR DETAILS

ARTICLE TYPE www. rsc.org/xxxxxx | XXXXXXXX

Carrier scattering and relaxation dynamics in n-type $In_{0.83}Ga_{0.17}As$ as a function of temperature and doping density

Yingjie Ma,[a] Yi Gu,[a] Yonggang Zhang,*[a] Xingyou Chen,[a] Suping Xi,[a] Zoltan Boldizsar,[b] Li Huang[b] and Li Zhou[a]

The carrier scattering and relaxation dynamics in n-type $In_{0.83}Ga_{0.17}As$ ternary alloy are investigated by measuring the temperature dependent electron Hall mobilities and the hole lifetimes as a function of doping density. The dominant scattering mechanisms in temperature ranges of T<80 K, 80<T<120 K, and 120<T<300 K in lightly doped $In_{0.83}Ga_{0.17}As$ are found to be the impurity scattering, the alloy disorder scattering and the phonon scattering, respectively, while in heavily doped $In_{0.83}Ga_{0.17}As$ the alloy scattering dominates over the whole measured temperature range. By fitting the measured temperature dependent carrier lifetimes, the dominant carrier relaxation mechanisms in lightly doped $In_{0.83}Ga_{0.17}As$ are identified to be the radiative and the Shockley-Read-Hall for samples grown on InP and GaAs substrates, respectively. The lifetime in heavily doped $In_{0.83}Ga_{0.17}As$ is below 10 ns with an Auger dominated recombination. Lastly, photoluminescence as well as the light absorption measurements are performed, showing that the grown lightly doped $In_{0.83}Ga_{0.17}As$ has a high optical quality comparable to the lattice-matched $In_{0.53}Ga_{0.47}As$.

1 Introduction

Indium (In)-rich $In_xGa_{1-x}As$ ternary alloys ($0.53 \leq x \leq 1$) are of great interest in many areas of near infrared optoelectronic devices and high speed electronic devices, e.g. quantum well lasers[1], wavelength-extended infrared photodetectors[2], photovoltaic junctions[3], thermophotovoltaic energy converters[4] and high electron mobility transistors (HEMTs)[5], which benefits from the wide tunable band gaps of 0.36-0.74 eV and the higher electron mobility in In-rich $In_xGa_{1-x}As$ materials. Due to the lack of naturally lattice-matched substrates, In-rich $In_xGa_{1-x}As$ films are generally grown on lattice-mismatched InP or GaAs substrates via composition graded $In_xGa_{1-x}As$[6], $InAs_xP_{1-x}$[7] or $In_xAl_{1-x}As$[8] metamorphic buffer layers, leading to an inherently high residual threading dislocation density on the order of 10^7-10^9 cm^{-2} in the epitaxial layer. The strain[9] as well as the optical properties[10,11] in In-rich $In_xGa_{1-x}As$ layers have been studied and given progressive understanding of the epitaxial growth. However, in contrast to the $In_{0.53}Ga_{0.47}As$ lattice-matched to InP, so far only very limited data on the transport and lifetime properties have been reported in In-rich $In_xGa_{1-x}As$[12–16]. Also, those data show a large inconsistency possibly owing to the different sample structures, background doping levels and strain conditions. The carrier scattering and recombination dynamics has not been well understood yet. E.g. the mechanisms of suppression of the high dark current in PIN photodetectors based on $In_{0.83}Ga_{0.17}As$ absorbers remain uncertain[17–19]. The design and optimization of device performances based on In-rich $In_xGa_{1-x}As$ remain a big challenge owing to the insufficient understanding on material properties and the physics in it.

[a] State Key Laboratory of Functional Materials for Informatics, Shanghai Institute of Microsystem and Information Technology, Chinese Academy of Sciences, 865 Chang Ning Rd., Shanghai 200050, China. E-mail: ygzhang@mail.sim.ac.cn
[b] SEMILAB Semiconductor Physics Laboratory Co. Ltd., Prielle Kornelia str. 2, H-1117 Budapest, Hungary

Carrier mobility and minority carrier lifetime are crucial material parameters for both material grower and device fabricators to not only determine the quality of grown epilayer itself but also design and predict the device performance before device fabrication. For $In_{0.53}Ga_{0.47}As$, the mobility and lifetime properties in both p- and n-type materials have been extensively studied[20–24]. Different carrier scattering mechanisms, including ionized impurity scattering, alloy scattering and phonon scattering dominating in different temperature ranges respectively, have been determined[20]. Carrier relaxation mechanisms, including the Shockley-Read-Hall (SRH) effect, the radiative recombination and the Auger recombination, dominating at various doping densities have been also identified[24]. Compared to $In_{0.53}Ga_{0.47}As$, the carrier scattering and relaxation processes in the metamorphically grown In-rich $In_xGa_{1-x}As$ are more complicated owing to increased lattice distortion, especially in the high doping regime. A suppressed carrier mobility and lifetime in In-rich $In_xGa_{1-x}As$ is foreseeable considering the increased defect density, which has not been investigated experimentally or theoretically so far. In those senses, an extensive study on the carrier mobility and lifetime in In-rich $In_xGa_{1-x}As$ films over a wide range of temperature and doping is necessary to not only understand the fundamental physics but also improve the device performances.

In this paper, the carrier scattering and relaxation dynamic-

Journal of Materials Chemistry C Accepted Manuscript

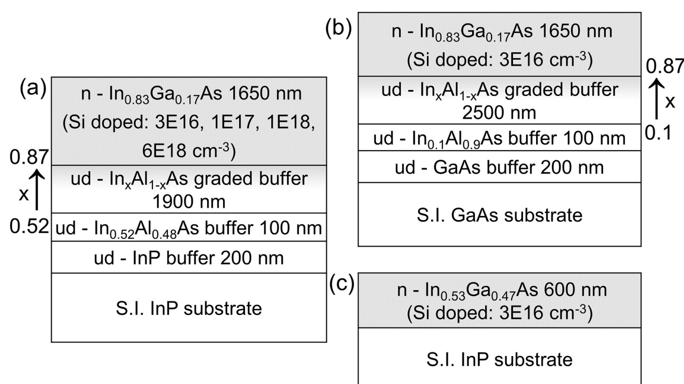

Fig. 1 Schematic epitaxial layer structures of $In_{0.83}Ga_{0.17}As$ grown on (a) InP and (b) GaAs substrates, and (c) $In_{0.53}Ga_{0.47}As$ grown on InP substrate.

s in n-type $In_{0.83}Ga_{0.17}As$ are identified for the first time by using temperature dependent characterizations of the majority carrier mobility and minority carrier lifetime as a function of doping density. The dominant carrier scattering and relaxation mechanisms in different temperature ranges and different doping density regimes are determined by fitting the measured temperature dependent electron Hall mobilities and hole lifetimes. Moreover, photoluminescence (PL) as well as light absorption measurements are performed, showing that the grown lightly doped $In_{0.83}Ga_{0.17}As$ has a high optical quality comparable to the lattice-matched $In_{0.53}Ga_{0.47}As$.

2 Sample preparation

In the growth of In-rich $In_{0.83}Ga_{0.17}As$ on InP substrate, normally a buffer structure is needed to release the strain and reach a full relaxation. An ideal buffer structure should have negligible contribution in the characterization of electrical and optical properties of the grown films to ensure high measurement accuracy. Previously [11,25], we have shown that the composition graded $In_xAl_{1-x}As$ layer has suitable buffer effects. It also has been found that unintentionally doped $In_{0.52}Al_{0.48}As$ or metamorphic $In_xAl_{1-x}As$ buffer layers show all high resistive features, mainly because of the background doping and carrier compensation effects in those Aluminum containing materials. The parallel conductance effects of the buffer structure in the Hall or microwave photoconductive decay (μ-PCD) measurements could be suppressed effectively and therefore $In_xAl_{1-x}As$ is a better buffer material than $In_xGa_{1-x}As$ or $InAs_xP_{1-x}$. Moreover, $In_xAl_{1-x}As$ has a larger bandgap than $In_xGa_{1-x}As$ and thus the buffer layer is transparent in absorption measurement at concerned wavelength band [10].

Epitaxial $In_{0.83}Ga_{0.17}As$ layers were grown using a VG Semicon V80H gas source molecular beam epitaxy (GSMBE) system. Si was used as the n-type dopant. As shown in Fig. 1(a), $In_{0.83}Ga_{0.17}As$ layers with a thickness of 1650 nm were grown on semi-insulating (S. I.) InP (001) epi-ready substrate with three undoped (ud) buffer layers which in turn consist of a 200-nm-thick InP, a 100-nm-thick $In_{0.52}Al_{0.48}As$ and a 1900-nm-thick composition graded metamorphic $In_xAl_{1-x}As$ (x was increased from 0.52 to 0.87 for a compositional overshoot to increase the residual strain relaxation degree in $In_{0.83}Ga_{0.17}As$). Four $In_{0.83}Ga_{0.17}As$ samples with nominal Si doping densities of 3×10^{16}, 1×10^{17}, 1×10^{18} and 6×10^{18} cm^{-3} were grown, which are referred as S83a, S83b, S83c and S83d, respectively. A 1650-nm-thick $In_{0.83}Ga_{0.17}As$ reference sample on S.I. GaAs (001) epi-ready substrate with a similar layer structure to S83a and a nominal Si doping density of 3×10^{16} cm^{-3} was also grown (refereed as S83r), as shown in Fig. 1(b). The large lattice mismatch between the GaAs substrate and the epi-layer significantly increases the strain in $In_{0.83}Ga_{0.17}As$ and induces much more threading dislocations, which will help to understand the influences of defect on the carrier scattering and recombination processes. Another reference sample of a 600-nm-thick $In_{0.53}Ga_{0.47}As$ layer was grown lattice-matched on InP substrate with a nominal Si doping density of 3×10^{16} cm^{-3} (referred as S53r), as shown in Fig. 1(c). A list on the material parameters as well as the measured and deduced 300 K physical properties of those samples is given in Table 1.

3 Results and discussion

3.1 Hall mobility

The temperature dependent free-carrier concentration and the electron Hall mobility were measured in a Quantum Design model-6000 physical property measurement system (PPMS) using the Van der Pauw-Hall method. The measured carrier densities (N_D) for those samples show less than 30% variation from the nominal values. Figure 2(a) illustrates the temperature dependent electron Hall mobility data. It is seen that the electron mobility decreases by a factor of ∼80% for S83 a-d with the doping density increases from 3×10^{16} to 6×10^{18} cm^{-3}. Noteworthy is that the mobility in S83a shows a temperature dependency of first increase and then decrease with decreasing temperature, which is similar to that in lattice-matched $In_{0.53}Ga_{0.47}As$.[20] Such dependency attenuates with increasing doping density. Similar temperature tendencies were observed for the two lightly doped reference samples of S83r and S53r, in which the carrier mobility was decreased by a factor of ∼20% and ∼80% compared to that in S83a, respectively. Figure 2(b) shows the measured electron Hall mobilities of $In_{0.83}Ga_{0.17}As$ layers as a function of N_D at 10, 100 and 300 K. Data points for the S83r and S53r are also shown. It is clearly seen that the mobilities decrease with N_D and the

This journal is © The Royal Society of Chemistry [year]
Journal of Materials Chemistry C Accepted Manuscript

Table 1 A list on the material parameters as well as the measured and deduced 300 K physical properties of the grown $In_{0.83}Ga_{0.17}As$ with different doping densities (referred as S83a, S83b, S83c and S83d) and the two reference samples (referred as S53r and S83r).

Sample	Material	Sub.	Hall N_D (cm^{-3})	Hall μ_e ($cm^2V^{-1}s^{-1}$)	E_{alloy} (eV)	τ_S (ns)	L_d (μm)	PL peak E (meV)
S83a	$In_{0.83}Ga_{0.17}As$	InP	1.0×10^{16}	13300	0.67	32.6	8.83	496.8
S83b	$In_{0.83}Ga_{0.17}As$	InP	1.2×10^{17}	10600	0.64	<10	undetected	499.5
S83c	$In_{0.83}Ga_{0.17}As$	InP	1.3×10^{18}	5800	0.71	<10	undetected	574.7
S83d	$In_{0.83}Ga_{0.17}As$	InP	5.9×10^{18}	3000	0.88	<10	undetected	700.6
S53r	$In_{0.53}Ga_{0.47}As$	InP	1.3×10^{16}	3300	0.65	29.8	5.02	733.5
S83r	$In_{0.83}Ga_{0.17}As$	GaAs	3.8×10^{16}	11000	0.56	12.5	4.95	undetected

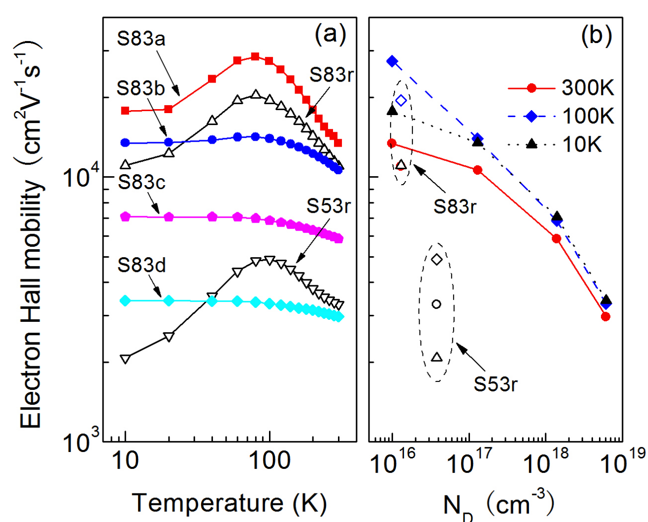

Fig. 2 (a) Measured temperature dependent electron Hall motilities of S83 a-d and the two reference samples of S83r and S53r. (b) The measured Hall mobilities of $In_{0.83}Ga_{0.17}As$ layers as a function of N_D at 10, 100 and 300 K. Data points for S83r and S53r are also given.

mobilities at different temperatures tend to converge at high doping densities. The temperature dependency is stronger for S53r than that for S83 a-d and r.

It has been reported that several carrier scattering mechanisms dominating in different temperature ranges, respectively, are coexisted in lattice-matched $In_{0.53}Ga_{0.47}As$ and lightly mismatched $In_xGa_{1-x}As$ alloys [20,21]. The carrier mobility is a result of competition among those scattering mechanisms. The observed similar temperature dependency of S83a to S53r could also be elucidated by the competition among the ionized impurity scattering, the alloy scattering and the LO phonon scattering which dominate in the temperature ranges of about 0-50, 50-120, 120-350 K, respectively [20]. For a more quantitative interpretation, we have fitted the temperature dependence of the measured Hall mobilities using equation:

$$\frac{1}{\mu_{\rm measured}} = \frac{1}{\mu_{\rm impurity}} + \frac{1}{\mu_{\rm alloy}} + \frac{1}{\mu_{\rm phonon}} \quad (1)$$

where $\mu_{measured}$ is the measured mobility, $\mu_{impurity}$, μ_{alloy} and μ_{phonon} are the contribution parts from ionized impurity scattering, alloy disorder scattering, and phonon scattering, respectively. Those three terms are identified from their temperature dependence as $\mu_{\rm impurity} = AT^{3/2}$,$\mu_{\rm alloy} = BT^{-1/2}$, and $\mu_{\rm phonon} = C(\frac{E_g}{k_BT})^{-3/2}\exp(\frac{\gamma}{1+\gamma}\cdot\frac{E_g}{k_BT})$, respectively, where T is temperature, A, B and C are fitting parameters. E_g is the bandgap, k_B is the Boltzmann constant, γ is the ratio of electron and hole effective mass (γ=14.5 for $In_{0.83}Ga_{0.17}As$). Other minor scattering mechanisms, e.g. the neutral impurity scattering, the inter-carrier scattering and etc., are omitted in the fitting process.

Table 2 Fitting parameters for the measured temperature dependent Hall motilities of samples S83 a-d, S53r and S83r.

	A ($\times10^5$) ($cm^2/VsK^{3/2}$)	B ($\times10^3$) ($cm^2K^{1/2}/Vs$)	C ($\times10^8$) (cm^2/Vs)
S83a	3.0±0.08	0.2±0.02	0.7±0.01
S83b	2.3±0.05	5.7±0.2	-
S83c	1.8±0.03	5.5±0.05	-
S83d	1.2±0.02	2.9±0.02	-
S53r	0.6±0	0.03±0	4.4±0
S83r	2.2±0.06	0.1±0.01	1.2±0.05

Figures 3(a)-(c) show the fitting results for S53r, S83a and S83d, respectively. Fitting parameters for the measured tem-

Journal of Materials Chemistry C Accepted Manuscript

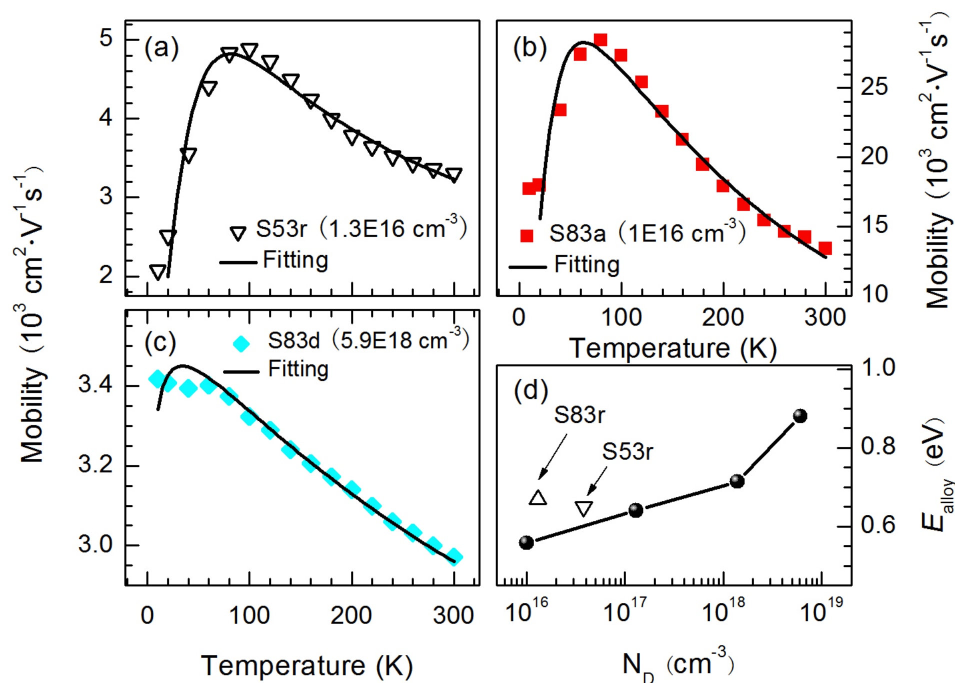

Fig. 3 Fitting results of the measured Hall mobilities for (a) S53r (b) S83a and (c) S83d using equation 1. (d) The deduced E_{alloy} for $In_{0.83}Ga_{0.17}As$ layers as a function of N_D. Data points for the two reference samples are also given.

perature dependent Hall motilities of samples S83 a-d, S53r and S83r are listed in Table 2. From Figs. 3(a) and (b), it is seen that equation 1 gives good fittings of the measured mobilities for both S53r and S83a at the low doping level of 3×10^{16} cm^{-3}. At the high doping level of 6×10^{18} cm^{-3} (S83d), the fitting curve shows a good agreement at T>80 K and a relatively large discrepancy at T<80 K, as shown in Fig. 3(c). From the fitting parameters, it is found that the dominated scattering mechanisms in temperature ranges of T<80 K, 80<T<120 K, and 120<T<300 K in S83a are the impurity scattering, the alloy scattering and the phonon scattering, respectively, which is similar to that in lattice-matched S53r. It is also found that the contribution of alloy scattering increases over the whole measured temperature range for heavily doped $In_{0.83}Ga_{0.17}As$ samples while the other two scattering contributions decrease. In order to understand more quantitatively, the alloy disorder potential E_{alloy} is estimated using the equation[26]:

$$\mu_{\text{alloy}} = \frac{(2\pi)^{1/2} e\hbar^4 N_a}{3(k_B T)^{1/2} m_e^{*5/2} E_{alloy}^2 x(1-x)} \tag{2}$$

where e is the electron charge, $\hbar$ is the reduced Planck's constant $\hbar$=h/2π, N_a is the density of alloy scattering centers, m_e^* is the electron effective mass (m_e^*=(0.51-0.1x)m_0 for $In_xGa_{1-x}As$), E_{alloy} is the depth of the random potential well and x is the alloy fraction. Figure 3(d) shows the deduced E_{alloy} for $In_{0.83}Ga_{0.17}As$ at 300 K as a function of N_D. Data points for the two reference samples are also shown. E_{alloy} shows a monotonic increase with increasing N_D, suggesting an increased alloy scattering contribution in the carrier transport in $In_{0.83}Ga_{0.17}As$ at high doping levels. The E_{alloy} for S83r shows a slight increase as compared to S83a with the same doping density, which is probably due to an increased lattice defect density. Those E_{alloy} results also indicate the increase of Si dopant density in $In_xGa_{1-x}As$ alloy would cause an increased lattice distortion and hence increased alloy disordering scattering.

3.2 Minority carrier lifetime

For high-speed device applications based on In-rich $In_xGa_{1-x}As$, it is important to measure and know the carrier lifetimes at different doping regimes and temperatures. μ-PCD minority carrier lifetime measurement is a technique based on the photoconductivity dependent microwave reflectance[27,28]. The minority carrier (i.e. the hole) lifetimes of the n-type $In_{0.83}Ga_{0.17}As$ and the reference samples were measured by using a μ-PCD system (WT-2000) of SEMILAB with an overall temporal resolution of ~10 ns. Surface charge passivation technique was applied to eliminate the surface recombination lifetime as well as the characteristic time for d-

This journal is © The Royal Society of Chemistry [year]
Journal of Materials Chemistry C Accepted Manuscript

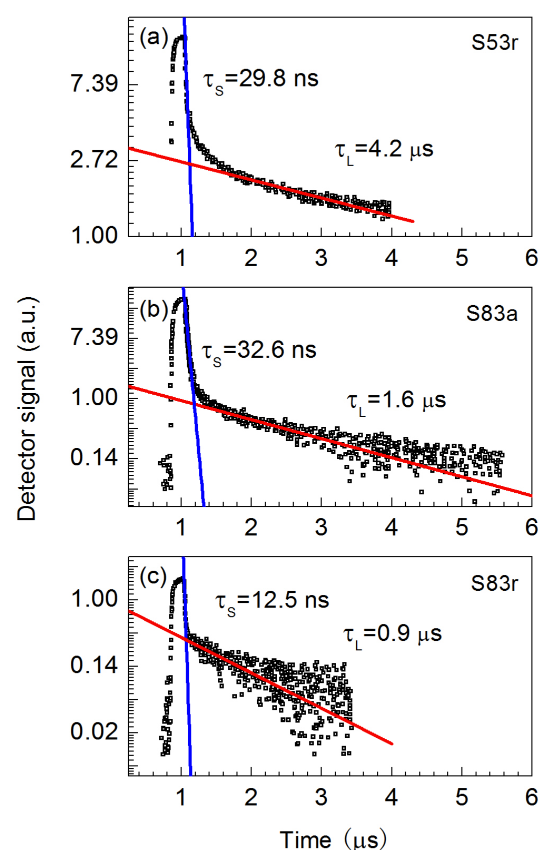

Fig. 4 Measured RT μ-PCD transient signal (in ln scale) on (a) S53r, (b) S83a and (c) S83r. The fitted short (τ_S) and long (τ_L) lifetimes are also illustrated.

iffusion to the surface from the bulk, and thus to give directly the bulk recombination lifetime[29]. Figures 4(a)-(c) show the measured room temperature (RT) transient signals (in unit of mV) of S53r, S83a and S83r, respectively. Samples have shown strong multiexponential feature with short (τ_S) and long (τ_L) lifetime parts. τ_S and τ_L are defined by fitting the decay curves with the expression of $I(t) = \alpha e^{-t/\tau_S}$ and $I(t) = \beta e^{-t/\tau_L}$, respectively, where α and β are fitting parameters.

Generally, the interpretation of the physical origins of the fitted two decay times is not readily, and is closely related to the material properties. The generated non-equilibrium carriers in the direct bandgap bulk $In_xGa_{1-x}As$ relax via radiative and nonradiative recombination processes, including the interband radiative recombination, the defect related SRH recombination and the Auger recombination[24,30]. Among those three channels the radiative recombination is a relatively fast process while the two other nonradiative recombinations could contain both fast and slow components[22–24,31]. Both τ_S and τ_L are results of the competition among those recombination mechanisms. We suggest that τ_L mainly originated from the nonradiative recombination channels, including the doping density related Auger effect and the crystal defect density related SRH effect. The short lifetime part τ_S is suggested to originate from the competition between the radiative and the nonradiative recombination processes, which is case sensitive depending on the intrinsic material properties (e.g. the band structure and the doping level) as well as its crystal quality (e.g. defect density).

From the fittings in Fig. 4, it is found that the τ_S are 29.8, 32.6 and 12.5 ns, and the τ_L are 4.2, 1.6 and 0.9 μs for S53r, S83a and S83r, respectively. The even higher τ_S for S83a as compared to S53r indicates that grown lightly doped $In_{0.83}Ga_{0.17}As$ has a high crystal quality comparable to the lightly doped $In_{0.53}Ga_{0.47}As$. However, the τ_L for S83a is reduced compared to S53r, indicating the slow recombination processes in $In_{0.83}Ga_{0.17}As$ play less important roles than that in $In_{0.53}Ga_{0.47}As$. This could be associated with the different defect types in them. The τ_S for S83r is lower compared to S83a, which suggests that the increased defect density in S83r increases the nonradiative recombination centers and less carriers relax via rapid radiative recombination processes, while the suppressed τ_L indicates an overall degraded crystal quality. The transit signals of $In_{0.83}Ga_{0.17}As$ with higher doping densities (S83 b-d) were too weak to be detected, indicating their lifetimes are severely suppressed and are less than the system temporal resolution of $\sim$10 ns.

To quantitatively determine the dominant recombination mechanism in those materials, other advanced measurements must be exploited. Temperature dependent lifetime measurements have been recently demonstrated to be a robust route in determining the dominant carrier recombination mechanisms in narrow-bandgap compound semiconductors[32–35]. By fitting the measured temperature dependent lifetimes using the SRH, radiative and Auger recombination equations, the contributions of the various recombination mechanisms could be distinguished and the dominated carrier relaxation mechanism could also be identified.

In this work, the temperature dependent τ_S of holes in 77-300 K for S53r, S83a and S83r were measured and fitted, as illustrated in Fig. 5(a). It is found that τ_S in the $In_{0.83}Ga_{0.17}As$ samples (S83a and S83r) are lower than that in the lattice-matched $In_{0.53}Ga_{0.47}As$ sample (S53r) over the whole measured temperature range. S83r shows a lower τ_S compared to S83a. Moreover, τ_S shows opposite temperature dependencies for S83a and S83r, i.e. τ_S increases and decreases with increasing T for S83a and S83r, respectively. The τ_S tendency of S83r is similar to S53r. The temperature dependent τ_L was not quantitatively fitted in measurements. However, it was qualitatively found that τ_L monotonically increases with decreasing temperature for all the three samples of S53r, S83a

Journal of Materials Chemistry C Accepted Manuscript

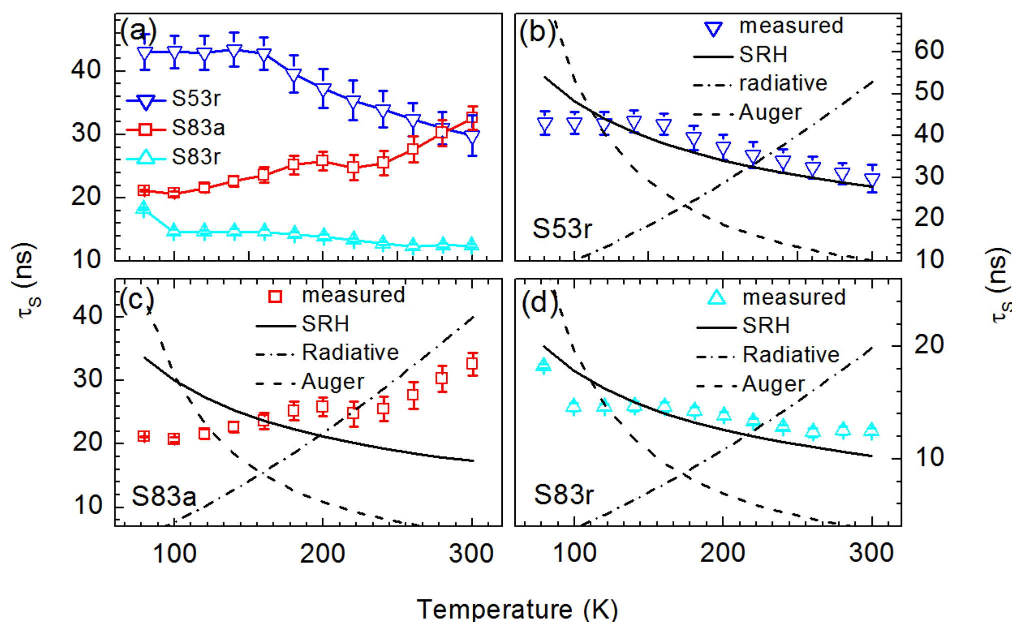

Fig. 5 (a) Temperature dependent hole τ_S for samples S83a, S53r and S83r. (b)-(d) The separately fitted temperature dependent lifetime components of SRH, radiative and Auger for S53r, S83a and S83r, respectively, using equation 3.

and S83r. I.e. τ_L follows a similar temperature dependency to τ_S for S53r, indicating a SRH dominated recombination[36]. The temperature dependent τ_S is fitted by the law of addition of reciprocal lifetimes[35] given by

$$\tau_S^{-1} = \tau_{SRH}^{-1} + \tau_R^{-1} + \tau_A^{-1} \tag{3}$$

where τ_{SRH}, τ_R and τ_A are the SRH lifetime, the radiative lifetime and the Auger lifetime, respectively. Those three components have temperature dependencies, respectively, of $\tau_{SRH} = P_1 T^{-1/2}$, $\tau_R = P_2 T^{3/2}$ and $\tau_A = P_3(\frac{E_g}{k_B T})^{3/2}\exp(\frac{1+2\gamma}{1+\gamma}\cdot\frac{E_g}{k_B T})$, where P_1, P_2 and P_3 are fitting parameters[32,34,36]. Figures 5(b)-(d) show the separately fitted temperature dependent lifetime components of SRH, radiative and Auger for S53r, S83a and S83r, respectively. The fitting parameters are listed in Table 3. It is seen that τ_S follows mainly the SRH lifetime trend for S53r. The radiative recombination contribution increases at T<170 K (Fig. 5(b)) while the SRH recombination plays the dominant role at T>170 K. This result may suggest that the point defects in lattice-matched $In_{0.53}Ga_{0.47}As$ alloys are partially deactivated at low temperatures. For S83a, τ_S follows mainly the radiative lifetime trend at T>200 K (Fig. 5(c)). At T<200 K, τ_S is a competition between the SRH and the radiative recombination. Such characteristic is possibly associated with the smaller bandgap and thus stronger electron-hole wave-function overlap, which give rise to an easier radiative emission. However, details remain unclear, further theoretical analyses are still needed. For S83r, τ_S follows mainly the SRH lifetime trend over the whole measured temperature range, which is likely due to the increased lattice defect density. Similar to S53r, the radiative recombination notably affect τ_S at T<170 K, which is also tentatively attributed to the deactivated lattice defects at low temperatures. Auger recombination plays a minor role for all three samples, which is reasonable since Auger recombination only dominates at high free carrier concentration regime[31]. This also explains the measured sub-10 ns lifetime for S83 b-d with doping densities larger than 3×10^{16} cm^{-3}, in which the nonradiative Auger recombination is expected to play the dominant role.

Table 3 Fitting parameters for the measured temperature dependent hole τ_S of samples S53r, S83a and S83r.

	P_1 $(s\cdot K^{1/2})$	P_2 $(\times10^{-3})$ $(s\cdot K^{-3/2})$	P_3 $(\times10^{4})$ (s)
S53r	482.7±16.7	10.2±2.1	5.3±0.9
S83a	304.8±32.1	7.7±0.9	3.1±0.8
S83r	178.2±6.3	3.8±0.7	1.9±0.3

This journal is © The Royal Society of Chemistry [year]
Journal of Materials Chemistry C Accepted Manuscript

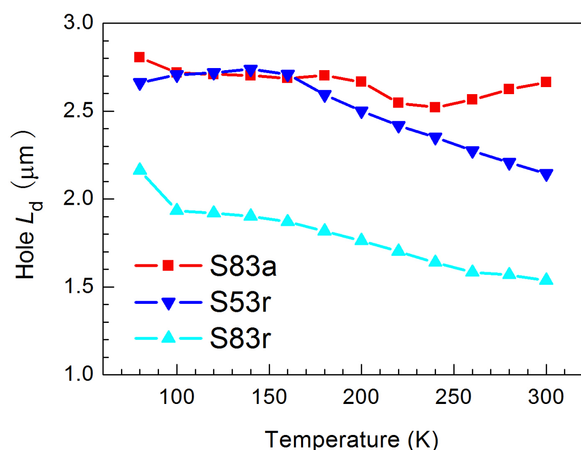

Fig. 6 Calculated hole L_d for S83a, S53r and S83r as a function of temperature.

3.3 Carrier diffusion length

Minority carrier diffusion length (L_d) is another important material parameter for minority-based optoelectronic device modeling and optimization, and also provides insight into the physics of carrier scattering. A larger L_d benefits more photo-generated carriers to arrive at the electrodes, leading to a higher quantum efficiency. For a full characterization, the hole L_d in S53r, S83a and S83r are deduced using

$$L_d = (D_p \tau_S)^{1/2} \quad (4)$$

where D_p is the hole diffusion coefficient $D_p = \frac{k_B T}{q} \mu_p$, μ_p is the hole mobility. The minority carrier mobility in $In_xGa_{1-x}As$ alloy is estimated using a empirical mobility model[37]

$$\mu_p(N,T) = \mu_{\min} + \frac{\mu_{\max}(300/T)^{\theta_1} - \mu_{\min}}{1 + (\frac{N_D}{N_{ref}(T/300)^{\theta_2}})^{\lambda}} \quad (5)$$

where $\mu_p(N,T)$ is the minority carrier mobility, N_D is the doping density, $\mu_{\min}$, $\mu_{\max}$ and N_{ref} are calculation parameters at 300 K. θ_1, θ_2 and λ are empirical parameters. For calculation of hole mobility in n-type $In_{0.83}Ga_{0.17}As$ and $In_{0.53}Ga_{0.47}As$, those empirical parameters are listed in Table 4. Considering the relatively high background doping level in our growth system, $\mu_{\max}$ and $\mu_{\min}$ values are reduced to be ∼1/4 of high purity materials as a conservative estimate. Figure 6 shows the deduced hole L_d as a function of temperature. It is found that S83a has a L_d of about 2.7 μm which is not strongly temperature dependent. In contrast, S83r and S53r have a smaller L_d of about 1.6-2.2 and 2.2-2.8 μm, respectively. Noteworthy is that both S53r and S83r show a negative temperature dependence, which might be intrinsically related to the similar carrier scattering (Fig. 2) and recombination (SRH dominated, Figs. 5(b) and (d)) mechanisms. The temperature-insensitive L_d has been also observed in undoped and lightly doped InGaP ternary alloys[38]. The dominant carrier scattering mechanisms at higher and lower temperatures in them are identified to be phonon scattering and alloy scattering, respectively[38], which is similar to that in S83a. The larger L_d in S83a is attributed to the higher mobility and the longer carrier lifetime than the two reference samples. The obviously decreased L_d for S83r compared to S83a suggests an increased defect density would drastically shorten the carrier L_d. It has been reported that the hole L_d in n-type $In_{0.53}Ga_{0.47}As$ doped to 1.4×16 cm^{-3} is determined to be ∼2.5 μm by measuring the short-circuit photocurrent[39]. Considering the rough minority carrier mobility model used here, it is worth pointing out that there might be error to some level of the calculated absolute value of L_d in figure 6. However, their relative magnitudes as well as temperature dependencies are suggested to be reasonable.

3.4 Photoluminescence and light absorption coefficient

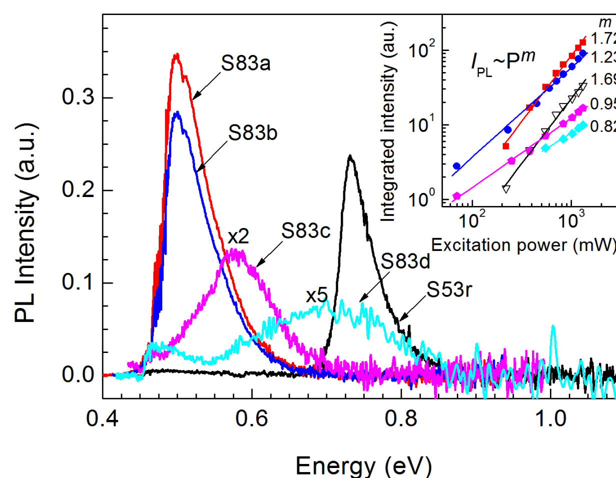

Fig. 7 Measured RT PL spectra of the $In_{0.83}Ga_{0.17}As$ films with different doping densities (S83 a-d) and the S53r under an excitation power of 500 mW. Inset: integrated PL intensity as a function of excitation power. Lines are linear fittings. The extracted *m* values are given accordingly.

RT PL measurements of the $In_{0.83}Ga_{0.17}As$ films with different doping densities (S83 a-d) and the two reference samples (S53r and S83r) were conducted in a Fourier transform infrared spectroscopy (FTIR) spectrometer[40,41]. A semiconductor laser (532 nm) was used as the excitation source. The PL spectra were recorded by a liquid-nitrogen cooled InSb detector. Figure 7 shows the RT PL spectra measured at an exci-

Journal of Materials Chemistry C Accepted Manuscript

Table 4 The calculation parameters for n-type $In_{0.83}Ga_{0.17}As$ and $In_{0.53}Ga_{0.47}As$ used in the mobility model.

	μ_{max} ($cm^2V^{-1}s^{-1}$)	μ_{min} ($cm^2V^{-1}s^{-1}$)	N_{ref} (cm^{-3})	λ	θ_1	θ_2
$In_{0.83}Ga_{0.17}As$	104	3.6	2.49×10^{17}	0.435	1.9	3.0
$In_{0.53}Ga_{0.47}As$	80	2.5	4.9×10^{17}	0.403	1.59	3.0

tation power of 500 mW. The PL intensity for $In_{0.83}Ga_{0.17}As$ shows a monotonic decrease with increasing doping density. This is mainly because of the increased Auger effect at high doping levels. Besides, the high-density Si dopants in $In_{0.83}Ga_{0.17}As$ would also induce impurity defect bands in the energy gap, which act as nonradiative recombination centers. S83r showed a PL intensity lower than the system detection limit, indicating that the increased dislocation density in $In_{0.83}Ga_{0.17}As$ also dramatically degrades its optical quality. The PL peak energies show blueshifts and the peaks broaden with the increase of doping density, which are attributed to the energy level filling and degeneration at high doping levels. Inset of Fig. 7 shows the power dependence of the integrated intensity of PL peaks (I_{PL}) for those samples. The linear relationship between the I_{PL} and the excitation power (P) can be fitted by $I_{PL}\sim P^m$, where m is a good figure of merit to assess material quality for device applications[42]. Larger m means less nonradiative defect density and higher spontaneous emission quantum efficiency and vice versa[43]. The extracted m is also given in the inset. It is found that m decreases with increasing doping density. The m for the S83a (m=1.72) is in close proximity to the S53r (m=1.69), indicating the grown $In_{0.83}Ga_{0.17}As$ layer has a high optical quality comparable to the lattice-matched $In_{0.53}Ga_{0.47}As$ at low doping levels.

The RT infrared light absorption spectra of S83 a-d, S53r and S83r were also acquired by using FTIR with corresponding background reference samples. Results are shown in Fig. 8. S83r showed an undetected light absorption signal and is not shown, which proves again the increased dislocation density dramatically degrades the optical quality and should be avoided whenever possible. From Fig. 8, it is seen that the absorption coefficient (α) shows a remarkable decrease when the doping density exceeds 1×10^{17} cm^{-3} (S83c). Further increase of the doping density causes a dramatically decrement of α to 10^2-10^3 cm^{-1} (S83d), especially at the low energy side, clearly demonstrates the degradation of absorption at high doping levels. Increased free carrier absorption may be expected in those heavily doped $In_{0.83}Ga_{0.17}As$ samples. Noteworthy is that S83a shows α of $\sim10^4$ cm^{-1} comparable to S53r, being another evidence of the good optical quality of the grown lightly doped $In_{0.83}Ga_{0.17}As$.

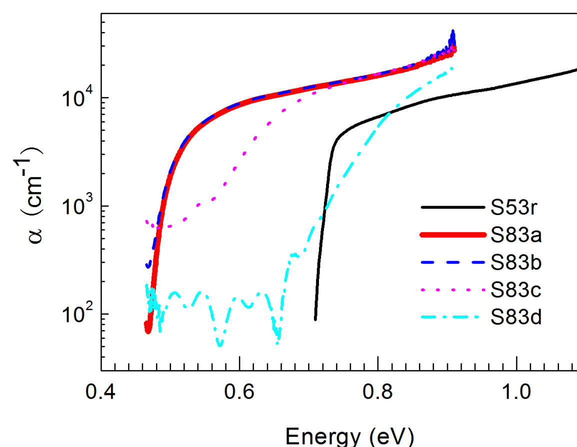

Fig. 8 Measured RT infrared light absorption spectra of the $In_{0.83}Ga_{0.17}As$ films with different doping densities (S83 a-d) and the S53r.

4 Conclusions

In conclusion, we systematically investigated the carrier mobility and lifetime properties in MBE grown n-type $In_{0.83}Ga_{0.17}As$ layers as a function of temperature and doping density. The dominant scattering mechanisms in temperature ranges of T<80 K, 80<T<120 K, and 120<T<300 K in lightly doped $In_{0.83}Ga_{0.17}As$ are found to be the impurity scattering, the alloy disorder scattering and the phonon scattering, respectively, while in heavily doped $In_{0.83}Ga_{0.17}As$ the contribution of alloy scattering increases over the whole measured temperature range. The dominant carrier relaxation mechanisms in lightly doped $In_{0.83}Ga_{0.17}As$ are identified to be the radiative the SRH for samples grown on InP and GaAs substrates, respectively. The lifetime in heavily doped $In_{0.83}Ga_{0.17}As$ is below 10 ns with an Auger dominated recombination. PL and light absorption measurements results show that the grown lightly doped $In_{0.83}Ga_{0.17}As$ has a high optical quality comparable to the lattice-matched $In_{0.53}Ga_{0.47}As$. Heavy Si doping in In-rich $In_xGa_{1-x}As$ would dramatically lower its carrier mobility and lifetime as well as its optical quality. Those results are quite important for device

This journal is © The Royal Society of Chemistry [year]

Journal of Materials Chemistry C Accepted Manuscript

designs based on In-rich $In_xGa_{1-x}As$ and could be generalized to other In-rich III-V ternary alloys.

5 Acknowledgments

This work was supported by the National Basic Research Program of China under grant No. 2012CB619202, the National Natural Science Foundation of China under grant Nos. 61275113, 61204133, 61334004 and 61405232, and the China Postdoctoral Science Foundation under grant No. 2013M531234.

References

1 T. Sato, M. Mitsuhara, T. Watanabe, K. Kasaya, T. Takeshita and Y. Kondo, *IEEE J Sel. Top. Quant.*, 2007, **13**, 1079–1083.
2 Y. Zhang, Y. Gu, Z. Tian, A. Li, X. Zhu and Y. Zheng, *Infrared Phys. Techn.*, 2007, **51**, 316–321.
3 M. W. Wanlass, J. S. Ward, K. A. Emery, M. M. Al-Jassim, K. M. Jones and T. J. Coutts, *Sol. Energy Mater. Sol. Cells*, 1996, **41/42**, 405.
4 M. W. Wanlass, J. J. Carapella, A. Duda, K. Emery, L. Gedvilas, T. Moriarty, S. Ward, J. Webb, X. Wu and C. S. Murray, *AIP Conf. Proc.*, 1998, **460**, 132.
5 D. H. Kim, J. A. D. Alamo, J. H. Lee and K. S. Seo, *IEEE T Electron Dev.*, 2007, **54**, 2606–2613.
6 A. Moseley, M. Scott, A. Moore and R. Wallis, *Electron. Lett.*, 1986, **22**, 1206–1207.
7 G. H. Olsen, *Proc. SPIE*, 1988, **972**, 279.
8 L. Zimmermann, J. John, S. Degroote, G. Borghs, C. V. Hoof and S. Nemeth, *Appl. Phys. Lett.*, 2003, **82**, 2838.
9 P. Y. Chang, L. Zeng, X. Y. Liu and K. L. Wei, International Conference on Simulation of Semiconductor Processes and Devices (SISPAD), 2013, pp. 388–391.
10 L. Zhou, Y. Zhang, Y. Gu, X. Chen, Y. Cao and H. Li, *J. Alloy Compd.*, 2013, **576**, 336–340.
11 X. Y. Chen, Y. G. Zhang, Y. Gu, L. Zhou, Y. Y. Cao, X. Fang and H. Li, *J. Cryst. Growth*, 75-80, **393**, 2014.
12 S. ichiro Gozua, T. Kita, Y. Sato, S. Yamada and M. Tomizawa, *J. Cryst. Growth*, 2001, **227-228**, 155–160.
13 F. Capotondi, G. Biasiol, D. Ercolani, V. Grillo, E. Carlino, F. Romanato and L. Sorba, *Thin Solid Films*, 2005, **484**, 400–407.
14 Y. K. Yeo, A. C. Bergstrom, R. L. Hengehold, J. W. Wei, S. Guha, L. P. Gonzalez, G. Rajagopalan and M.-Y. Ryu, *J. Korean Phys.Soc.*, 2011, **58**, 1267.
15 S.-K. Hong, H.-G. Lee, J.-J. Lee, S.-G. Kim, K.-E. Pyun and H.-M. Park, *J. Cryst. Growth*, 1996, **169**, 435–442.
16 X. Wallart, B. Pinsard and F. Mollot, *Appl. Phys. Lett.*, 2005, **97**, 053706.
17 R. W. M. Hoogeveen, R. J. van der A and A. P. H. Goede, *Infrared Phys. Technol.*, 2001, **42**, 1–16.
18 L. Zhou, Y. G. Zhang, X. Y. Chen, Y. Gu, H. S. B. Y. Li, Y. Y. Cao and S. P. Xi, *J. Phys. D: Appl. Phys.*, 2014, **47**, 085107.
19 X. Ji, B. Liu, H. Tang, X. Yang, X. Li, H. Gong, B. Shen, P. Han and F. Yan, *AIP Adv.*, 2014, **4**, 087135.
20 J. D. OLIVER, J. L. F. EASTMAN, P. D. KIRCHNER and W. J. SCHAFF, *J. Cryst. Growth.*, 1981, **54**, 64–68.
21 T. Matsuoka, E. Kobayashi, K. Taniguchi, C. Hamaguichi and S. Sasa, *Jpn. J. Appl. Phys.*, 1990, **29**, 2017–2025.
22 D. Vignaud, J. F. Lampin, E. Lefebvre, M. Zaknoune and F. Mollot, *Appl. Phys. Lett.*, 2002, **80**, 4151–4153.
23 D. Vignaud, D. A. Yarekha, J. F. Lampin, M. Zaknoune, S. Godey and F. Mollot, *Appl. Phys. Lett.*, 2007, **90**, 242104.
24 R. K. Ahrenkiel, R. Elling, S. Johnston and M. Wanlass, *Appl. Phys. Lett.*, 1998, **72**, 3470–3472.
25 Y. Zhang, Y. Gu, K. Wang, A. Li and C. Li, *Semicond. Sci. Technol.*, 2008, **23**, 125029.
26 J. Tietjen and L. R. Weisberg, *Appl. Phys. Lett.*, 1965, **7**, 261.
27 V. Grivickas, D. Noreika and J. A. Tellefsen, *Sov. Phys. Collect.*, 1989, **29**, 591.
28 S. Rein, R. Hull, R. M. O. Jr., J. Parisi and H. Warlimont, *Lifetime Spectroscopy*, Springer, New York, 2010, p. 59.
29 T. Pavelka, . Pap, P. Kenesei, M. Varga, F. Novinics, M. Tallin, G. Borionetti, G. Guaglio, M. Pfeffer and E. Don, *ECS Transactions*, 2009, **25**, 129–137.
30 R. K. Ahrenkiel, S. W. Johnston, J. D. Webb, L. M. Gedvilas and J. J. Carapella, *Appl. Phys. Lett.*, 2001, **78**, 1092–1094.
31 W. K. Metzger, M. W. Wanlass, R. J. Ellingson, R. K. Ahrenkiel and J. J. Carapella, *Appl. Phys. Lett.*, 2001, **79**, 3272–3274.
32 B. V. Olson, E. A. Shaner, J. K. Kim, J. F. Klem, S. D. Hawkins, M. E. Flatt and T. F. Boggess, *Appl. Phys. Lett.*, 2013, **103**, 052106.
33 B. V. Olson, E. A. Shaner, J. K. Kim, J. F. Klem, S. D. Hawkins, L. M. Murray, J. P. Prineas, M. E. Flatt and T. F. Boggess, *Appl. Phys. Lett.*, 2012, **101**, 092109.
34 E. H. Steenbergen, B. C. Connelly, G. D. Metcalfe, H. Shen, M. Wraback, D. Lubyshev, Y. Qiu, J. M. Fastenau, A. W. K. Liu, S. Elhamri, O. O. Cellek and Y.-H. Zhang, *Appl. Phys. Lett.*, 2011, **99**, 251110.
35 Y. Chang, C. H. Grein, J. Zhao, C. R. Becker, M. E. Flatte, P.-K. Liao, F. Aqariden and S. Sivananthan, *Appl. Phys. Lett.*, 2008, **93**, 192111.
36 R. K. Ahrenkiel and M. S. Lundstrom, *Semiconductors and Semimetals*, Academic, New York, 1993, vol. 39, pp. 39–150.
37 M. Sotoodeh, A. H. Khalid and A. A. Rezazadeh, *J. Appl. Phys.*, 2000, **87**, 2890–2900.
38 F. J. Schultes, T. Christian, R. Jones-Albertus, E. Pickett, K. Alberi, B. Fluegel, T. Liu, P. Misra, A. Sukiasyan, H. Yuen and N. M. Haegel, *Appl. Phys. Lett.*, 2013, **103**, 242106.
39 M. M. Tashima, L. W. Cook and G. E. Stillman, *Appl. Phys. Lett.*, 1981, **39**, 960–961.
40 Y. G. Zhang, Y. Gu, K. Wang, X. Fang, A. Z. Li and K. H. Liu, *Rev. Sci. Instrum.*, 2012, **83**, 053106.
41 Y. G. Zhang, S. P. Xi, L. Zhou, Y. Gu, X. Y. Chen and Y. J. Ma, *J. Infrared Millim. Waves*, 2015, in press.
42 D. Ding, S. R. Johnson, J.-B. Wang, S.-Q. Yu and Y.-H. Zhang, *Proc. of SPIE*, 2007, **6841**, 68410D.
43 Q. Dai, M. F. Schubert, M. H. Kim, J. K. Kim, E. F. Schubert, D. D. Koleske, M. H. Crawford, S. R. Lee, A. J. Fischer, G. Thaler and M. A. Banas, *Appl. Phys. Lett.*, 2009, **94**, 111109.

This journal is © The Royal Society of Chemistry [year]

Journal of Materials Chemistry C Accepted Manuscript

The carrier scattering and relaxation dynamics in n-type $In_{0.83}Ga_{0.17}As$ as a function of temperature and doping density were studied.

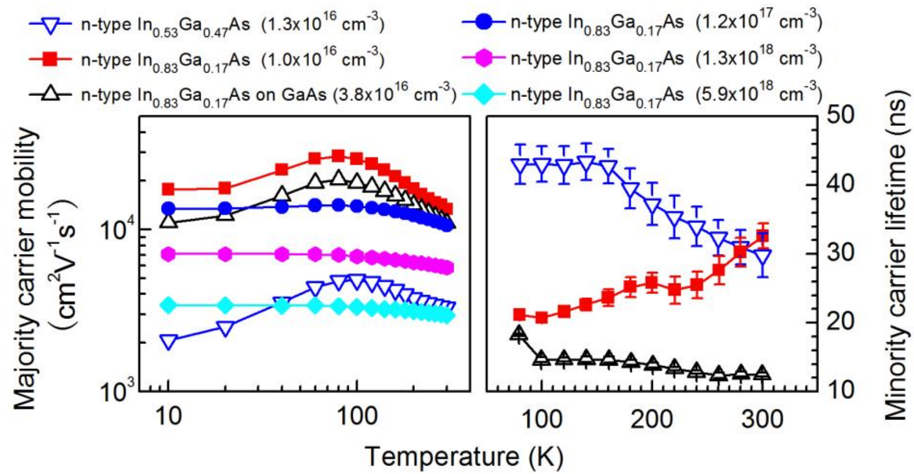

Journal of Materials Chemistry C Accepted Manuscript